



## **Dynamic Process for Biosorption of Cadmium in Aqueous Solution using Column Packed with Lignocellulosic Material**

**Candelaria Tejada-Tovar<sup>1</sup>, Angel Villabona-Ortíz<sup>2</sup>, Diofanor Acevedo\*<sup>3</sup>,  
Angelica Cabarcas<sup>4</sup>, Cristian Benitez<sup>5</sup>**

<sup>1,2,4,5</sup>Faculty of Engineering, Chemical Engineering program, Research Group IDAB, University of Cartagena Av. El Consulado, St. 30 No. 48-152. Colombia.

<sup>3</sup>Faculty of Engineering, Research Group Innovation, Agricultural and Agro-industrial Development, University of Cartagena Av. El Consulado, St. 30 No. 48-152. Colombia.

**Abstract :** In the present investigation, the biosorption process for the removal of Cadmium in synthetic waters was adjusted on a pilot scale using cocoa shells as a biosorbent. This was obtained by calculating the experimental values using the response surface methodology (RSM) and an experimental design  $3^3$ , varying the feed rate, initial solution concentration and bed height, where the respective rupture curve was determined, using the Adams-Bohart, Thomas, Yoon-Nelson and Dose Response models to describe the behaviour of the column and obtain the kinetic parameters. The model that best fitted the experimental data and described the rupture curve was the Dose-response model, with an  $R^2$  value of 0.9979, followed by the Yoon-Nelson model with an  $R^2$  value of 0.9503, the Adams-Bohart model with an  $R^2$  value of 0.9246, and finally the Thomas model with an  $R^2$  value of 0.8728, which reached 0.9246. The cocoa shell is shown as a good precursor to generate adsorbent at low cost of heavy metals.

**Keywords :** Biosorption, Cadmium, Breakthrough curve, Thomas model.

### **1. Introduction**

Industrial wastewater contains large quantities of potentially toxic heavy metal ions that are discharged into wastewater treatment plants. Conventional methods of treatment to remove heavy metal ions from wastewater include precipitation, flotation, ion exchange, membrane-related methods and electrochemical techniques [1]. Precipitation is often used for high concentrations of heavy metal ions, but ion exchange is used for low concentrations of metal ions in effluents. Ion exchange resins are expensive. The development of low-cost sorbents with a high capacity to remove or recover heavy metal ions has recently become a crucial element [2, 3].

The use of biosorption to remove heavy metal ions generates the advantages mentioned above. Two types of biosorbents are often used to remove heavy metal ions from the solution: agricultural residues and micro-organisms [4]. The use of biosorbents produced from agricultural waste is a simple method to remove

heavy metals from wastewater [5]. The use of agricultural waste products such as fruit peels, shells, straw and coconut as biosorbents is a simple and low-cost method of removing heavy metals from wastewater. Numerous researchers have observed that fiber-rich agricultural residues produce biosorbents, with studies in batch systems being a precedent for assessing the feasibility of biosorption processes for real-world applications, continuous biosorption studies in packaged bed columns would be more useful [5, 6].

A wide variety of mathematical models with different levels of complexity have been used to describe and predict rupture curves of an adsorption column in liquid and gas phase systems, to investigate the metal adsorption mechanism, allowing some of these models to describe the dynamics of the solute adsorption rate, evaluating the closeness between the experimental data and those calculated with the model is evaluated by correlation coefficients.

Long et al., [7] predicted the rupture curves for adsorption of Pb (II) in aqueous solution on common mushroom (*Agaricus bisporus*), using the models of Adams, Thomas and Yoon-Nelson. Similarly, other authors have modeled rupture curves and determined the efficiency of adsorption of emerging contaminants such as methylene blue, phenol from a refinery wastewater using pyrolytic activated carbon and evaluated the effect of initial contaminant concentration and flow [8, 9]. On the other hand, using orange peel, uranium (VI) was removed, studying the bed heights, initial concentrations and flow rates, comparing the experimental results with those produced by the Thomas, Yoon-Nelson and Adams-Bohart models, the first two being the best fit [10].

The adsorption efficiency of the eucalyptus bark was also tested in the removal of methylene blue in aqueous solution, performing a series of experiments in a continuous fixed-bed system to determine rupture curves and evaluate the effect of variable inlet flow (10-15 mL/min), initial dye concentration (50-100 mg L<sup>-1</sup>) and adsorbent bed height (10-15 cm), finding that high bed height, low flow rate and initial high dye concentration were the best conditions for maximum dye adsorption and that Thomas, Yoon-Nelson and BDST models are suitable for describing the dynamic behaviour of the column with respect to the parameters under study [11].

Valencia-Ríos and Castellar-Ortega [12] predicted the rupture curves for lead removal (II) using granular activated carbon in a packed bed column under dynamic conditions at 27°C, evaluating the effect of bed height (1-10cm), flow and initial concentration of the pollutant on rupture time and adsorption capacity at pH 4. Column performance was improved by increasing the height of the activated carbon bed and decreasing the volumetric flow and initial concentration. The experimental data of the rupture curves were adjusted to the BDST (Bed Depth Service Time), Clark and Wolborska models, the first one being the one that better adjusted the experimental data.

Chao et al., [13] used grapefruit shells (*Citrus maxima*), passion fruit (*Passiflora edulis*) and sugar cane bagasse (*Saccharum officinarum*) to produce bioadsorbent to remove Copper (II), Cadmium (II), Nickel (II) and Lead (II) ions in a fixed-bed column. The bioadsorbent material was characterized by scanning electron microscopy, zeta potential analysis, Fourier Transform Infrared Spectroscopy (FTIR) and ion exchange capability, while adsorption capacities were determined using Thomas's kinetic model for different pH and flow rates, resulting in biosorbents having carboxylic acid groups, which function as interchangeable cation and complexing sites to remove heavy metals with a large adsorption capacity, which showed decreased as the flow rate increased and decreased as the pH of the solution increased from 4 to 6. In addition, it was shown that the adsorption process was produced by ion exchange and complexing, the latter being the primary adsorption mechanism, with grapefruit peel being the one that produced the best ion retention results.

Cocoa cob waste (*Theobroma cacao*) was used in the removal of lead and cadmium ions present in synthetic aqueous solution by means of a fixed bed system, determining the effect of bed height on the adsorption capacity of these contaminants, maintaining constant pH, flow velocity and initial metal concentration. The adsorption tests showed a removal of 91,32 and 87,80% respectively for Pb and Cd after 4,5 h. When evaluating the Thomas, Dose-Response, Adams-Bohart and BDST mathematical models, it was found that for Thomas and Dose-Response, it was observed that the values of initial adsorption capacity,  $q_0$ , decreased as the height of the bed increased, this may have been due to slower mass transfer, lower concentration and increased adsorption capacity, while the Adams-Boh models were not. Volumetric adsorption capacity,  $N_0$ ,

decreases as the bioadsorbent in the column increases, which is an indicator that cocoa residues can be used for removal of heavy metals present in wastewater satisfactorily [14].

The use of a multi-metal binding biosorbent in the removal of cadmium, copper, lead and zinc was studied in a continuous fixed bed system, evaluating the effect of flow rate, metal concentration and bed height at pH  $5.5 \pm 0.1$  for a sample of synthetic wastewater. The maximum biosorption capacities of 38.25, 63.37, 108.12 and 35.23 mg/g for Cd, Cu, Pb and Zn, respectively, were reached at a bed height of 31 cm, a flow rate of 10 ml / min and an initial concentration of 20 mg/L. The Thomas model best described all the dynamic behavior of the column rather than the Yoon-Nelson Response Dose models. Finally, desorption studies indicated that the metal-loaded biosorbent could be used after three consecutive cycles of sorption, desorption and regeneration by the application of semi-simulated wastewater [15].

The objective of this research was to describe the behaviour of the column of a biosorption process for the elimination of Cadmium in synthetic waters at pilot scale using cocoa shells as a biosorbent, by constructing rupture curves using the models of Adams-Bohart, Thomas, Yoon-Nelson and Dose-Response, obtaining the corresponding kinetic parameters.

## 2. Experimental

### 2.1 Experimental design

In the present investigation, a  $3^3$  factorial design has been used. The optimum configuration of the operational parameters was then determined by the Response Surface Method (RSM) with which the respective rupture curve was constructed using the models of Adams-Bohart, Thomas, Yoon-Nelson and Response Dose as fit models to obtain the corresponding kinetic parameters. Three independent variables were worked on: three bed heights, three feed rates and three initial concentration values of Cadmium, which are shown in Table 1. In terms of the responses to be optimised, two have been selected: the percentage retained of Cadmium (%) and the biosorption capacity of Cadmium ( $q_e$ , mg g<sup>-1</sup>) [16].

**Table 1. Factorial type experimental design**

Factors	Experimental domain		
	(-1)	(0)	(+1)
X1: Feed flow rate (mL min <sup>-1</sup> )	4.5	6	7.5
X2: Initial concentration of metal (ppm)	40	100	160
X3: Bed height (g of biomass)	5	10	15

### 2.2. Experimental procedure

#### 2.2.1. Preparation of biomass

The cocoa shell was washed with distilled water to remove residues contained in it until the washing water has non-colouring at all, to remove impurities that may interfere with adsorption. It was then dried at 90°C for 24 h in an Esco furnace, the Isotherm<sup>®</sup>OFA-32-8 model. It was ground in a Corona brand knife mill for 20 min and sieved to obtain a particle size of 0.5 mm in a Shaker stainless steel AISI 316 stainless steel sieve. The resulting material was stored in airtight bags for later use as a bioadsorbent [17].

#### 2.2.2 Synthetic water preparation

To prepare the 10.3, 12.7 and 15.1 L of each synthetic solution of Cd (II) at 40, 100 and 160 ppm, 0.94, 1.16 and 1.38 g of Cadmium Sulphate Octahydrate were used. (3Cd SO<sub>4</sub> H<sub>2</sub>O) from Merck Chemicals for the solution of 40 ppm, 2.35, 2.90 and 3.44 g for the solution of 100 ppm and 3.76, 4.63 and 5.51 g for the solution of 160 ppm, taking into account its molecular weight and number of moles, in order to obtain a solution with a pH of 6.0 [3].

### 2.2.3. Experimental assembly

An experimental set-up was carried out by varying the height of the bed, the initial concentrations of synthetic water and the flow rate, using beds with 5,10 and 15 g of biomass, through which each synthetic water solution prepared is passed at concentrations of 40,100 and 160 ppm, with flow rates of 4,5, 6 and 7.5 mL min<sup>-1</sup>. This was done in a continuous system equipment which consists of a feed tank that receives synthetic water and is pumped into the system and stored. This assembly has a valve system that allows regulating the flow of inlet and outlet. In the end, samples were collected in properly labeled test tubes, which were analyzed with an atomic absorption spectrometer to measure the final concentration of Cadmium present in the respective aliquots [14].

### 2.2.4 Adjustment models: determination of kinetic parameters

After the collection of experimental data and obtaining one of the two response variables, which are: percentage retained of Cadmium (%) and biosorption capacity of Cadmium ( $q_e$ , mg g<sup>-1</sup>), the RSM was applied by comparing two factors (independent variables), leaving the third factor constant, with the retained percentage of Cadmium (% R). With this method it was possible to obtain the optimal parameters of the system, with which the rupture curve was generated[18].

To determine the model that best fits the system, a breakthrough curve was made with the operating conditions that yielded the optimum response value. According to the results obtained in the experiments, these conditions were: initial metal concentration of 100 ppm, flow rate of 4.5 mL min<sup>-1</sup> and bed height of 5 g of biomass [18]. Under these conditions, a final experiment was carried out, in which samples were taken every 60 min to complete a total of 420 min (7 h) and data were obtained on retained metal concentration. The next step was to obtain the rupture curve, graphing the time (t) with respect to the retained concentration on the initial concentration (C/C<sub>i</sub>) and apply the adjustment models in order to obtain the kinetic parameters of each one that best fits the system. This adjustment was made by non-linear regression to the Adams-Bohart, Thomas, Yoon-Nelson and Dose-Response models.

#### 2.2.4.1. Adams-Bohart model:

The fundamental equation describing the relationship between C/C<sub>i</sub> and t in a continuous system was established by Bohart and Adams in 1920 and, although originally applied to a gas-solid system, it has been widely used to describe and quantify other types of systems. This model assumes that sorption rate is proportional to the residual capacity of the solid and the concentration of the retained species and is used to describe the initial part of the rupture curve [14]. This model is described by the Equation 1:

$$\frac{C}{C_0} = \frac{\exp(K_{AB} C_0 t)}{\exp\left(\frac{K_{AB} N_0 L}{v}\right) - 1 + \exp(K_{AB} C_0 t)} \quad (1)$$

Where  $k_{AB}$  is the kinetic constant (L mg<sup>-1</sup> min<sup>-1</sup>),  $N_0$  is the maximum volumetric sorption capacity (mg L<sup>-1</sup>),  $C$  is the solution concentration in the liquid phase (mg L<sup>-1</sup>),  $v$  is the linear flow rate (cm min<sup>-1</sup>), and  $Z$  is the filling height in the column (cm).

#### 2.2.4.2 Thomas model:

The Thomas model is one of the most general and used to describe the behavior of the biosorption process in fixed bed columns. Its main limitation is that its derivation is based on second-order kinetics and considers that biosorption is not limited by chemical reaction but controlled by matter transfer at the interface. This discrepancy can lead to errors when this method is used to model biosorption processes under certain conditions [14]. This model is described by the Equation 2:

$$\frac{C}{C_0} = \frac{1}{1 + \exp\left[\frac{k_{Th}}{Q}(q_0 X - C_0 V)\right]} \quad (2)$$

Where  $k_{Th}$  is the Thomas velocity constant (mL/min? mg) and  $q_0$  is the maximum solvent concentration in the solid phase (mg/g).

### 2.2.4.3. Yoon-Nelson Model

Yoon and Nelson developed a relatively simple model aimed at adsorbing vapors or gases in activated carbon. This model assumes that the rate at which the adsorption probability for each adsorbate molecule decreases is proportional to the adsorption probability of the adsorbate and the probability that it is not adsorbed onto the adsorbent. The Yoon and Nelson model, in addition to being less complex than others, does not require data on adsorbate characteristics, adsorbent type or physical properties of the bed [8, 14]. The equation that represents this model is:

$$\frac{C}{C_0} = \frac{\exp(K_{YN}t - \tau K_{YN})}{1 + \exp(K_{YN}t - \tau K_{YN})} \quad (3)$$

Where  $k_{YN}$  is the Yoon-Nelson proportionality constant (min<sup>-1</sup>) and  $\tau$  is the time required to retain 50% of the initial adsorbate (min). It should be noted that the Yoon and Nelson model equation is mathematically analogous to the Thomas model equation shown in equation 2.

### 2.2.4.4. Dose-response Model

This model, which has been commonly used in pharmacology to describe different types of processes, is currently being used to describe spinal biosorption processes [19, 20, 21]. The general equation represented by this model is as follows:

$$\frac{C}{C_0} = 1 - \frac{1}{1 + \left(\frac{C_0 Q t}{q_0 X}\right)^a} \quad (4)$$

This model is of relative importance because it normally describes the complete rupture curve with great accuracy. However, it is difficult to relate empirical parameter "a" to experimental conditions, making it virtually impossible to change the scale of the system.

## 3. Results and discussions

The removal rate was calculated with the initial and final concentration after 7 h of equipment operation. The different combinations of each variable and its three levels were performed, with a total of 27 experiments divided into groups of 3 for a total of 9 days of experimentation, as shown in Table 2.

**Table 2. Data obtained in experimentation**

Day	Experiment	Initial concentration (ppm)	Height (g)	Flow rate (mL/min)	Final concentration (ppm)	Remotion (%)
1	1	40	5	4.5	3.35	91.49
	2	40	10	4.5	1.61	95.90
	3	40	15	4.5	0.91	97.69
2	4	40	5	6	2.57	93.47
	5	40	10	6	0.05	99.88
	6	40	15	6	0.13	99.68
3	7	40	5	7.5	5.45	86.15
	8	40	10	7.5	0.12	99.70
	9	40	15	7.5	0.08	99.79
4	10	100	5	4.5	52.82	46.09

	11	100	10	4.5	1.92	98.04
	12	100	15	4.5	0.22	99.77
5	13	100	5	6	59.52	39.26
	14	100	10	6	23.62	75.90
	15	100	15	6	0.15	99.84
6	16	100	5	7.5	54.26	44.63
	17	100	10	7.5	0.20	99.80
	18	100	15	7.5	0.04	99.96
7	19	160	5	4.5	92.17	41.35
	20	160	10	4.5	1.58	98.99
	21	160	15	4.5	0.91	99.42
8	22	160	5	6	121.59	22.63
	23	160	10	6	2.69	98.29
	24	160	15	6	0.18	99.88
9	25	160	5	7.5	114.77	26.97
	26	160	10	7.5	1.29	99.18
	27	160	15	7.5	0.18	99.88

Under these conditions, a final experiment was carried out, in which samples were taken from time to time to complete a total of 420 min (7 h) and data were obtained on retained metal concentration at each time. The next step was to obtain the rupture curve, graphing the time (t) with respect to the retained concentration on the initial concentration (C/Ci) and apply the kinetic models in order to obtain the parameters of each one that best fits the system. This adjustment was made by non-linear regression to the Adams-Bohart, Thomas, Yoon-Nelson and Dose-Response models.

### 3.1. Modelling of bed rupture curves

To describe the rupture curves of the column, the experimental data were adjusted to the kinetic models by means of non-linear regression to determine their corresponding parameters, statistical error (SS) and correlation coefficient (R<sup>2</sup>), obtaining the results shown in Table 3:

**Table 3. Adjustment parameters of the kinetic models**

Models	Parameters			
Adams-Bohart	$k_{AB}$ (L min <sup>-1</sup> mg <sup>-1</sup> )	$N_0$ (mg L <sup>-1</sup> )	SS	R <sup>2</sup>
	0.000032997	7056.35415	0.004273916	0.924569582
Thomas	$k_{Th}$ (mL min <sup>-1</sup> ·mg <sup>-1</sup> )	$q_0$ (mgg <sup>-1</sup> )	SS	R <sup>2</sup>
	0.087809146	15.37820933	0.007321326	0.872795039
Yoon-Nelson	$k_{YN}$ (min <sup>-1</sup> )	$\tau$ (min)	SS	R <sup>2</sup>
	0.005387719	367.1238391	0.002815837	0.95035305
Dose-Response	a	$q_0$ (mgg <sup>-1</sup> )	SS	R <sup>2</sup>
	1.429713701	4650.049314	0.000138266	0.997874932

As can be seen in the experimental and theoretical rupture curves shown in Figure 1 and the parameters of the corresponding models are presented in Table 3, the Adams-Bohart model adjusted the data in an acceptable manner, with a value of R<sup>2</sup> of 0.9246, which indicates a low but considerable discrepancy with the experimental values. The results of applying the Adams-Bohart model are very similar to those obtained in other research. On the other hand, the Yoon-Nelson model adjusted the data in an acceptable manner, with an R<sup>2</sup> value of 0.9503, slightly higher than the Adams-Bohart model. On the other hand, Thomas's model presented

considerable discrepancies with respect to the experimental data, with a value of  $R^2$  of 0.8728, being the model that less adjusted the system. As can be seen, the Dose-response model adjusted the data with great accuracy, with a value of  $R^2$  of 0.9979 and a very tiny statistical error, being the model that best adjusted the system, with a maximum adsorption capacity of  $8.1 \text{ mg g}^{-1}$ . As stated above, this model usually describes the complete rupture curve with great accuracy, which was evidenced by observing the parameter values and graph in Figure 1.

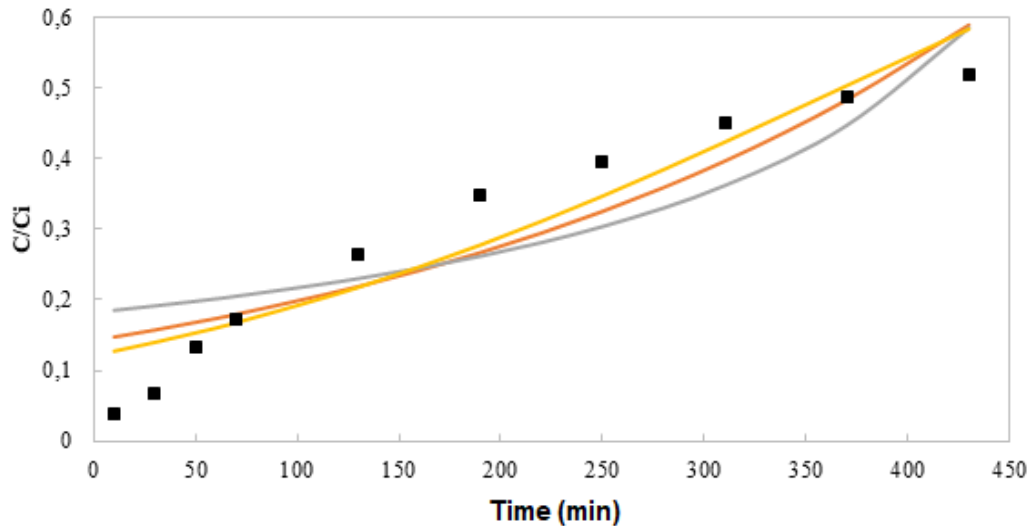


**Figure 1. Rupture curve and model adjustment. (■) Experimental data, (—) Adams Bohart, (—) Thomas, (—) Yoon-Nelson**

Previous investigations showed similar results to those of the present study, finding that Yoon-Nelson presented acceptable adjustment with  $R^2$  of 0.96 predetermining the constant adsorption rate, which increases with increased flow and decreases with increased depth of the bed. While the Dose-response model for all conditions tested was the most suitable to describe experimental data, with the highest determination coefficients, all above 0.996, minimizing errors presented when implementing this model with respect to the others evaluated [19]. This model has been widely applied to model the continuous adsorption of fixed bedding of inorganic contaminants, such as heavy metals, as well as organic pollutants, such as pharmaceuticals [22, 23].

Zhao and colleagues [24] used the Thomas and Dose-Response models to eliminate red by using residual biomass of wheat straw chemically modified with hexadecyltrimethylammonium bromide (CTAB) in continuous system, the Dose-response model was found to better fit the experimental data. Results similar to those found in other research [25, 26].

#### 4. Conclusion

After applying the response surface methodology, obtaining the optimal system parameters (initial metal concentration of 100ppm, flow rate  $4.5 \text{ mL min}^{-1}$  and bed height 5g) and generating the rupture curve, the Dose Response model was found to be the most effective in adjusting experimental data and describing the rupture curve, with a value of  $R^2$  of 0.9979, followed by the Yoon-Nelson model with an  $R^2$  value of 0.9503, the Adams-Bohart model with an  $R^2$  value of 0.9246 and finally the Thomas model with an  $R^2$  value of 0.8728, reaching a maximum contaminant adsorption capacity of  $8.1 \text{ mg g}^{-1}$ , showing that the cocoa shell is a good precursor to generate adsorbent of  $0.1 \text{ mg g}^{-1}$ .

#### References

1. Deniz, F. "Dye removal by almond shell residues: Studies on biosorption performance and process design", *Materials Science and Engineering*, vol. 33, no. 5, pp. 2821–2826, 2013.

2. Shanmugaprakash, M., Sivakumar, V. "Batch and fixed-bed column studies for biosorption of Zn(II) ions onto pongamia oil cake (*Pongamiapinnata*) from biodiesel oil extraction", *J. Environ. Manage.*, vol. 164, pp. 161–170, 2015.
3. Tejada, C., Herrera, A., & Ruiz, E. "Kinetic and isotherms of biosorption of Hg (II) using citric acid treated residual materials", *Ingeniería y competitividad*, vol. 18, no. 1, pp. 117-127, 2016.
4. Abdolali, A., Ngo, H.H., Guo, W.S., Zhou, J.L., Du, B., Wei, Q., Wang, X.C., Nguyen, P.D. "Characterization of a multi-metal binding biosorbent: chemical modification and desorption studies", *Bioresour. Technol.*, vol. 193, pp. 477–487, 2015.
5. Bhatnagar, A., Sillanpää, M., Witek-Krowiak, A. "Agricultural waste peels as versatile biomass for water purification – a review", *Chem. Eng. J.*, vol. 270, pp. 244–271, 2015.
6. Abdolali, A., Ngo, H.H., Guo, W.S., Lu, S., Chen, S.S., Nguyen, N.C., Zhang, X., Wang, J., Wu, Y. "A breakthrough biosorbent in removing heavy metals: equilibrium, kinetic, thermodynamic and mechanism analyses in a lab-scale study", *Sci. Total Environ.*, vol. 542, pp. 603–611, 2016.
7. Long Y, Lei D, Ni J, Ren Z, Chen C, Xu H. "Packed bed column studies on lead (II) removal from industrial wastewater by modified *Agaricus bisporus*". *Bioresource Technology*, vol. 152, pp. 457-63, 2014.
8. Makrigianni, V., Giannakas, A., Papadaki, M., Albanis, T., Konstantinou, I. "Fixed-bed adsorption study of methylene blue onto pyrolytic tire char", *Geophysical Research Abstracts*, vol. 30, 2016.
9. El-Naas, M.H., Alhaija, M.A., Al-Zuhair, S. "Evaluation of an activated carbon packed bed for the adsorption of phenols from petroleum refinery wastewater", *Environ Sci Pollut Res Int.* vol. 162, no. 3, pp. 997-1005, no. 2017.
10. Mahmoud, M.A. "Evaluation of Uranium Removal from Aqueous Solution using Orange Peels in the Fixed Bed System", *J Chem Eng Process Technol*, vol. 5, no. 5, pp. 1-5, 2014.
11. Tushar, S., Sharmeen, A., Ming, A. Adsorption performance of continuous fixed bed column for the removal of methylene blue (MB) dye using *Eucalyptus sheathiana* bark biomass. *Research on Chemical Intermediates*, vol. 42, no. 3, pp. 2343–2364, 2016.
12. Valencia-Ríos, J.S., Castellar-Ortega, G.C. "Predicción de las curvas de ruptura para la remoción de plomo (II) en disolución acuosa sobre carbón activado en una columna empacada", *Rev. Fac. Ing. Univ. Antioquia*, vol. 66, pp. 141-158, 2013.
13. Chao, H.P., Chang, C.C., Nieva, A. "Biosorption of heavy metals on *Citrus maxima* peel, passion fruit shell, and sugarcane bagasse in a fixed-bed column", *Journal of Industrial and Engineering Chemistry*, vol. 20, no. 5, pp. 3408-3414, 2014.
14. Lara J, Tejada C, Villabona A, Arrieta A. "Adsorción de plomo y cadmio en sistema continuo de lecho fijo sobre residuos de cacao", *Revista ION*, vol. 29, no. 2, pp. 111-122, 2016.
15. Adolali, A., Ngo, H.H., Guo, W., Zhou, J.L., Zhang, J., Liang, S., Chang, S.W., Nguyen, D.D., Liu, Y. "Application of a breakthrough biosorbent for removing heavy metals from synthetic and real wastewaters in a lab-scale continuous fixed-bed column", *Bioresource Technology*, vol. 229, pp. 78-87, 2017.
16. Amini, M. & Younesi, H. "Biosorption of Cd (II), Ni (II) and Pb (II) from aqueous solution by dried biomass of *Aspergillus niger*: Application of response surface methodology to the optimization of process parameters", *Clean*, vol. 37, no. 10, pp. 776-786, 2009.
17. Kyzas G, Deliyanni E, Matis K. "Activated carbons produced by pyrolysis of waste potato peels: Cobalt ions removal by adsorption", *Colloids and Surfaces A: Physicochemical and Engineering Aspects*, vol. 490, pp. 74-83, 2016.
18. Cabarcas, A. & Benítez, C. "Optimización de las variables del proceso en la biosorción de cadmio sobre cáscara de cacao en columna de lecho fijo", Diciembre 20. Universidad de Cartagena, 2016.
19. Ferreira, C.I.A., Calisto, V., Otero, M., Nadais, H., Esteves, V.I. "Fixed-bed adsorption of Tricaine Methanesulfonate onto pyrolysed paper mill sludge", *Aquacultural Engineering*, vol. 77, pp. 53-60, 2017.
20. Gusain, D., Kumar-Singh, P., Sharma, Y.C. "Kinetic and equilibrium modelling of adsorption of cadmium on nano crystalline zirconia using response surface methodology. *Environmental Nanotechnology, Monitoring & Management*, vol. 6, pp. 99-107, 2016.
21. Ribeiro-Nascimento, J., Sabadini-Santos, E., Carvalho, C., Annes-Keunecke, K., César, R., Bidone, E.D. "Bioaccumulation of heavy metals by shrimp (*Litopenaeus schmitti*): A dose–response approach for coastal resources management", *Marine Pollution Bulletin*, vol. 114, no. 2, pp. 1007-1013, 2017.
22. Singh, A., Kumar, D., Gaur, J.P. "Continuous metal removal from solution and industrial effluents using *Spirogyra* biomass-packed column reactor", *Water Res.*, vol. 46, pp. 779–788, 2012.



23. Katsigiannis, A., Noutsopoulos, C., Mantziaras, J., Gioldasi, M. "Removal of emerging pollutants through granular activated carbon", *Chem. Eng. J.*, vol. 280, pp. 49–57, 2015.
24. Zhao, B., Shang, Y., Xiao, W., Dou, C., Han, R. "Adsorption of Congo red from solution using cationic surfactant modified wheat straw in column model", *J. Env. Chem. Eng.*, Vol. 2, pp. 40-45, 2014.
25. Li, Y., Cao, L., Yang, C. "Promoting dynamic adsorption of Pb<sup>2+</sup> in a single pass flow using fibrous nano-TiO<sub>2</sub>/cellulose membranes", *Chem. Eng. J.*, vol. 283, pp. 1145-1153, 2016.
26. Muñoz, A.J., Espínola, F., Ruíz, E. "Removal of Pb(II) in a packed-bed column by a *Klebsiella* sp. 3S1 biofilm supported on porous ceramic Raschig rings", *J. Ind. Eng. Chem.*, vol. 40, pp. 118-127, 2016.

\*\*\*\*\*